Absorption cross sections, saturated vapor pressures, sublimation energies, and evaporation energies of some organic laser dye vapors

J. Schmidt and A. Penzkofer
Naturwissenschaftliche Fakultät II-Physik, Universität Regensburg, D-8400 Regensburg, Federal Republic of Germany

(Received 23 August 1988; accepted 27 March 1989)

A new technique of transmission measurement of overheated dye vapors is applied to determine absolute absorption cross-section spectra of three active dyes for vapor phase dye lasers. The investigated compounds are 1,4-di[2-(5-phenyloxazolyl)]-benzene (POPOP), 1,4-di[2-(4-methyl-5-phenyl-oxazolyl)]-benzene (dimethyl-POPOP), and 2,5-diphenylfuran (PPF). The vapor absorption spectra are compared with liquid solution spectra in order to obtain information on the dye–solvent interaction. The saturated vapor densities are determined by transmission measurements after knowing the absolute absorption cross-section spectra. The latent heats of sublimation, evaporation, and melting are derived by analyzing the dependences of the saturated vapor densities on the vapor temperature.

I. INTRODUCTION

The spectroscopic analysis of dye vapors gives molecule parameters free of solvent contributions.[1–9] The comparison of vapor spectra with solution spectra delivers information on the dye–solvent interaction.[4–10] The determination of absolute absorption cross-section spectra renders possible the measurement of thermodynamic dye properties like saturated vapor pressures and latent heats of sublimation, evaporation, and melting.[6–8,11,12] Dye vapors are applied to laser action[1–5] and nonlinear optics.[13–17] A thorough investigation of the dynamics of the laser action and of the nonlinear optical phenomena of dye vapors requires a detailed knowledge of the dye vapor densities and the absolute linear spectroscopic dye vapor parameters.

In this paper the technique of transmission measurement of overheated dye vapors[7] is applied to measure the absolute absorption cross-section spectra of the compounds 1,4-di[2-(5-phenyloxazolyl)]-benzene (POPOP)[4,5,11,17–38] and 2,5-diphenylfuran (PPF).[11,12,22,26,27,37,39] The absolute absorption cross-section spectrum of the dye 1,4-di[2-(4-methyl-5-phenyloxazolyl)]-benzene (dimethyl-POPOP)[2–4,21] has been determined previously.[7] The investigated dyes are active media for vapor phase dye lasers. Their structural formulas are shown in Fig. 1.

After knowing the absolute absorption cross sections, the saturated vapor number densities are determined by transmission measurements in cells with surplus dye content. Assuming an Arrhenius-type dye desorption mechanism latent heats of sublimation (temperature below melting point of dyes) and evaporation (temperature above melting point of dyes) are calculated. The energy differences between the latent heats of sublimation and evaporation provide the latent heats of melting.

II. FUNDAMENTALS

The theoretical fundamentals for the determination of (i) the absolute absorption cross sections, (ii) the saturated vapor densities, and (iii) the latent heats of phase changes, are derived in the following.

A. Determination of absolute absorption cross sections of dye vapors

The optical transmission of an overheated dye vapor in a cell is measured. (At the temperature of measurement no condensed dye is left in the cell.) The light transmission T at wavelength λ is

$$T(\lambda) = \exp[-\sigma(\lambda)N_v l] = \exp[-\alpha(\lambda)l], \quad (1)$$

$\sigma(\lambda)$ is the absorption cross section at wavelength λ, N_v is the number density (dimension cm^{-3}) of the overheated vapor, and l is the sample length. $\alpha(\lambda) = \sigma(\lambda)N_v$ is the absorption coefficient at wavelength λ.

The total number of dye molecules $N_0 V$ in the vapor cell is given by the molecules $N_v V$ in the vapor phase and the molecules $N_w A$ adsorbed at the cell walls. V is the cell volume and A is the inner wall surface of the cell. The dye vapor density is

$$N_v = N_0 - N_w A / V. \quad (2)$$

The number density of dye molecules N_w (dimension cm^{-2})

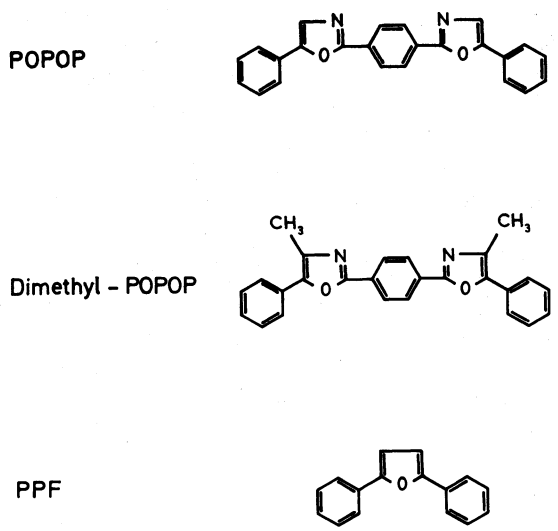

FIG. 1. Structural formulas of investigated dyes.

 0021-9606/89/151403-07$02.10

adsorbed to the walls is obtained by equating the rates of adsorption $n_{ad,w}$ and desorption $n_{des,w}$

The rate of adsorption is (Refs. 7 and 40, and page 874 of Ref. 41)

$$n_{ad,w} = n_{\downarrow} S_{wd} = \frac{p_v}{(2\pi m k\vartheta)^{1/2}} S_{wd} = N_v \left(\frac{k\vartheta}{2\pi m}\right)^{1/2} S_{wd}. \tag{3}$$

$n_{\downarrow}$ is the rate of vapor flow to the walls and is determined from gas kinetics. p_v is the dye vapor pressure. m is the mass of a dye molecule. k is the Boltzmann constant. ϑ is the cell temperature. S_{wd} is the dye–wall sticking coefficient denoting the fraction of incident molecules that are adsorbed at the wall. The last expression of Eq. (3) is obtained by application of the ideal gas equation

$$p_v = N_v k\vartheta. \tag{4}$$

The rate of desorption of dye molecules from the walls is

$$n_{des,w} = N_w \nu_{wd} \exp(-Q_{wd}/k\vartheta), \tag{5}$$

ν_{wd} is the attempt frequency of desorption of molecules from the wall and $\exp(-Q_{wd}/k\vartheta)$ gives the escape probability. Q_{wd} is the dye–wall desorption energy.

Equating the adsorption rate [Eq. (3)] and the desorption rate [Eq. (5)] gives

$$N_w = N_v \left(\frac{k\vartheta}{2\pi m}\right)^{1/2} \frac{S_{wd}}{\nu_{wd}} \exp\left(\frac{Q_{wd}}{k\vartheta}\right). \tag{6}$$

Insertion of this equation into Eq. (2) results in

$$N_v = N_0 \Big/ \left[1 + \frac{A}{V}\left(\frac{k\vartheta}{2\pi m}\right)^{1/2} \frac{S_{wd}}{\nu_{wd}} \exp\left(\frac{Q_{wd}}{k\vartheta}\right)\right] = \frac{N_0}{1 + \kappa_{wd}\vartheta^{1/2} \exp(Q_{wd}/k\vartheta)} \tag{7}$$

and, finally, Eq. (1) reads

$$T(\lambda) = \exp\left[-\frac{\sigma(\lambda) N_0 l}{1 + \kappa_{wd}\vartheta^{1/2} \exp(Q_{wd}/k\vartheta)}\right] = \exp[-\alpha(\lambda) l]. \tag{8}$$

The three unknown parameters, $\sigma(\lambda)$, κ_{wd}, and Q_{wd}, in Eq. (8) are determined by measuring the transmission $T(\lambda)$ through the overheated dye vapor cell at three different temperatures ϑ well above the saturation temperatures ϑ_S (for details see Ref. 7). ϑ_S is defined as the temperature where the amount of dye in a saturated vapor, $N_S V$, is equal to the dye inweighted, $N_0 V$, i.e., $N_0 = N_S$.

B. Determination of saturated dye vapor densities

Saturated dye vapors exist in vapor cells with surplus dye in the reservoir. The saturated vapor pressure p_s is determined by the equality of the rate of desorption and the rate of adsorption at the condensed dye surface.

The adsorption rate is

$$n_{ad} = n_{\downarrow} S = \frac{p_S}{(2\pi m k\vartheta_R)^{1/2}} S, \tag{9}$$

ϑ_R is the temperature of the dye reservoir and S is the dye–dye sticking coefficient.

The desorption rate is

$$n_{des} = n_{surf} \nu_{des} \exp(-Q_{des}/k\vartheta_R), \tag{10}$$

n_{surf} is the surface number density of dye molecules (dimension cm^{-2}). ν_{des} is the attempt frequency of desorption from the condensed dye and $\exp(-Q_{des}/k\vartheta_R)$ is the escape probability. Q_{des} is the dye–dye desorption energy.

The equality of adsorption of desorption rate results in

$$p_S = (2\pi m k\vartheta_R)^{1/2} \frac{\nu_{des}}{S} n_{surf} \exp\left(-\frac{Q_{des}}{k\vartheta_R}\right) = \kappa_{des} \vartheta_R^{1/2} \exp\left(-\frac{Q_{des}}{k\vartheta_R}\right). \tag{11}$$

The saturated dye vapor density in the vapor cell (temperature ϑ) is determined by use of the ideal gas equation ($p_S = N_S k\vartheta$). The result is

$$N_S = \frac{\kappa_{des} \vartheta_R^{1/2}}{k\vartheta} \exp\left(-\frac{Q_{des}}{k\vartheta_R}\right). \tag{12}$$

After knowing the absorption cross-section $\sigma(\lambda)$, the saturated vapor density N_S is determined experimentally by transmission measurements {Eq. (1): $T(\lambda) = \exp[-\sigma(\lambda) N_S l]$}. The desorption energies Q_{des} and the constants κ_{des} are determined by fitting Eq.12 to the experimental N_S points.

C. Determination of latent heats

The phase transition from solid to liquid (melting), solid to vapor (sublimation), and liquid to vapor (evaporation) follows a Carnot process with work $\Delta W = \Delta V dp_S$ and heat $\Delta Q = n_M \Lambda$. ΔV is the change of volume in the phase transition, Λ is the molar latent heat, and n_M is the number of moles transferred from one phase to another. The thermodynamic efficiency of the Carnot process is $\eta = \Delta W/\Delta Q = d\vartheta_R/\vartheta_R = \Delta V dp_S/(n_M \Lambda)$.

The change of saturated vapor pressure with temperature is

$$\frac{dp_S}{d\vartheta_R} = \frac{n_M \Lambda}{\vartheta_R \Delta V}. \tag{13}$$

Equation (13) is the Clapeyron equation (see, e.g., page 186 of Ref. 41). In the case of sublimation and evaporation it is $\Delta V = V(\text{vapor}) - V(\text{condensed}) \approx V(\text{vapor})$. Using the ideal gas equation one obtains $V(\text{vapor}) = n_M R\vartheta_R/p_S = n_M N_A k\vartheta_R/p_S$, and Eq. (13) transforms to the Clausius–Clapeyron equation:

$$\frac{dp_S}{d\vartheta_R} = \frac{\Lambda p_S}{N_A k \vartheta_R^2}, \tag{14}$$

R is the molar gas constant and N_A is the Avogadro constant. Calculating the temperature derivative of Eq. (11), the left-hand side of Eq. (14) reads

$$\frac{dp_S}{d\vartheta_R} = \left(\frac{1}{2\vartheta_R} + \frac{Q_{des}}{k\vartheta_R^2}\right) p_S. \tag{15}$$

Insertion of Eq. (15) into Eq. (14) leads to

$$\Lambda = \tfrac{1}{2} N_A k\vartheta_R + N_A Q_{des} \approx N_A Q_{des}. \tag{16}$$

More specific, the molar latent heat of evaporation Λ_e is

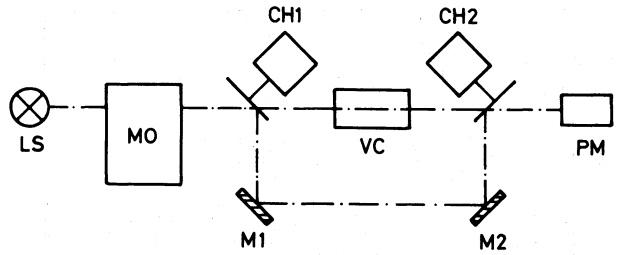

FIG. 2. Schematic experimental setup of absorption measurement in spectrophotometer. LS, light source. MO, monochromator. CH1 and CH2, light reflecting choppers. VC, vapor cell. M1 and M2, mirrors. PM, photomultiplier.

$\Lambda_e = N_A Q_e$ ($\vartheta_R > \vartheta_m$, ϑ_m melting temperature of dye), and the molar latent heat of sublimation Λ_s is $\Lambda_s = N_A Q_s$ ($\vartheta_R < \vartheta_m$). The latent heat of melting Λ_m is obtained by $\Lambda_m = \Lambda_s - \Lambda_e$.

III. EXPERIMENTAL

The optical transmissions of the dyes POPOP, dimethyl-POPOP, and PPF in the vapor phase and in the solvent cyclohexane are measured with a conventional spectrophotometer (Beckman type ACTA MIV). The schematic experimental setup is shown in Fig. 2. Details of the experimental arrangement and of the vapor cell are described in Ref. 7. The vapor cell temperature ϑ is kept approximately 15° higher than the reservoir temperature ϑ_R in order to avoid dye deposition at the vapor cell windows.

The absolute absorption cross-section spectra are derived from transmission measurements of overheated dyes at three different temperatures. The saturated vapor densities are obtained from transmission measurements with surplus dye in the reservoir.

IV. RESULTS

A. Absorption cross-section spectra

The absolute absorption cross-section spectrum of dimethyl-POPOP was determined in Ref. 7 and is not shown here.

Figures 3(a) and 4(a) show the applied temperature profiles to the vapor cells, and Figs. 3(b) and 4(b) give the corresponding absorption coefficient curves at the wavelengths of maximum S_0–S_1 absorption for POPOP and PPF,

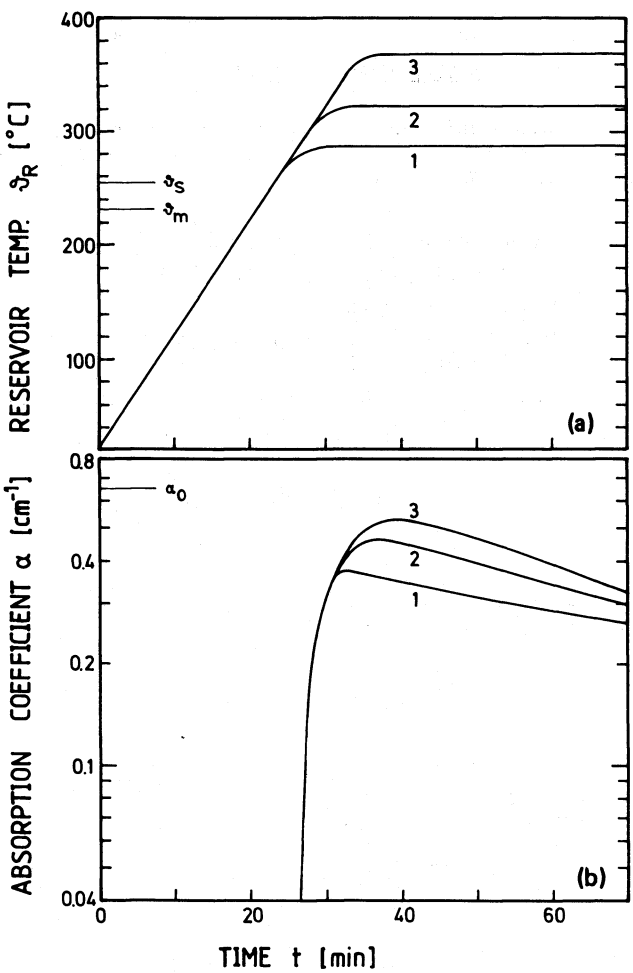

FIG. 3. Absorption coefficient measurement procedure for absorption cross-section determination. (a) Temperature profiles. (b) Corresponding absorption coefficients vs time at $\lambda = 322$ nm. Maximum dye number density is $N_0 = 4.3 \times 10^{15}$ cm^{-3}. α_0 is absorption coefficient corresponding to N_0. Dye is POPOP. Dye–wall desorption energy $Q_{wd} = 1.0 \times 10^{-19}$ J, coefficient $\kappa_{wd} = 10^{-8}$ Pa K$^{-1/2}$ (Ref. 7).

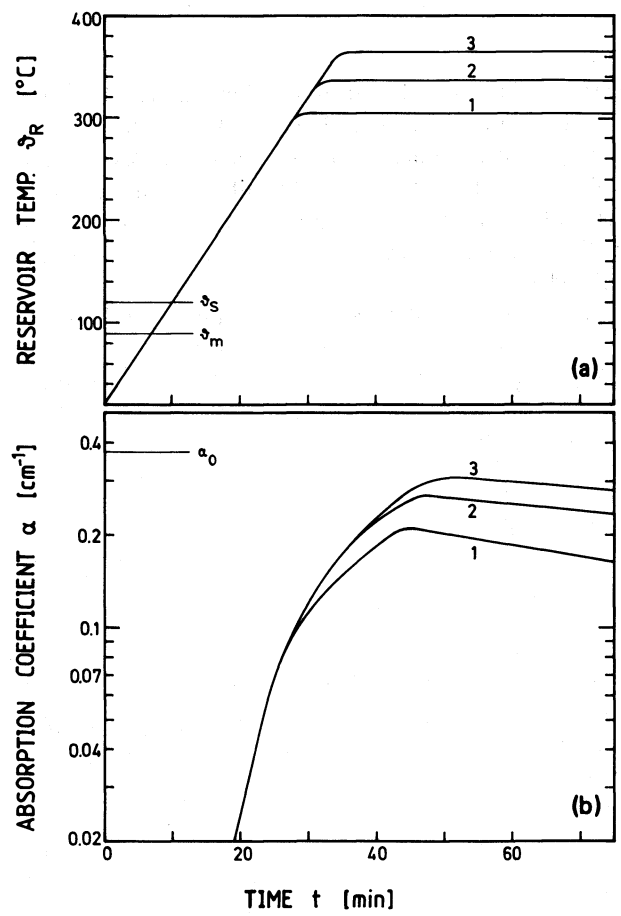

FIG. 4. Absorption coefficient analysis for absorption cross-section determination. (a) Temperature profiles. (b) Corresponding absorption coefficients vs time at $\lambda = 305$ nm. Maximum dye number density is $N_0 = 3.37 \times 10^{15}$ cm^{-3}. α_0 is the absorption coefficient corresponding to N_0. Dye is PPF. Dye–wall desorption energy $Q_{wd} = 1.3 \times 10^{-19}$ J, coefficient $\kappa_{wd} = 5 \times 10^{-9}$ Pa K$^{-1/2}$ (Ref. 7).

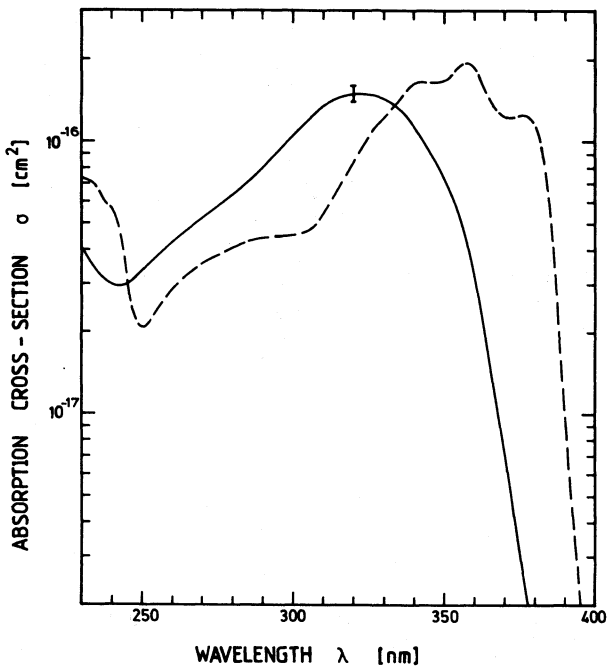

FIG. 5. Absorption cross-section spectra of POPOP. Dashed curve, dye dissolved in cyclohexane (concentration 10^{-4} mol/dm^3). Solid curve, dye vapor at $\vartheta_R = 250$ °C. Cell temperature ϑ is 15° higher than reservoir temperature ϑ_R.

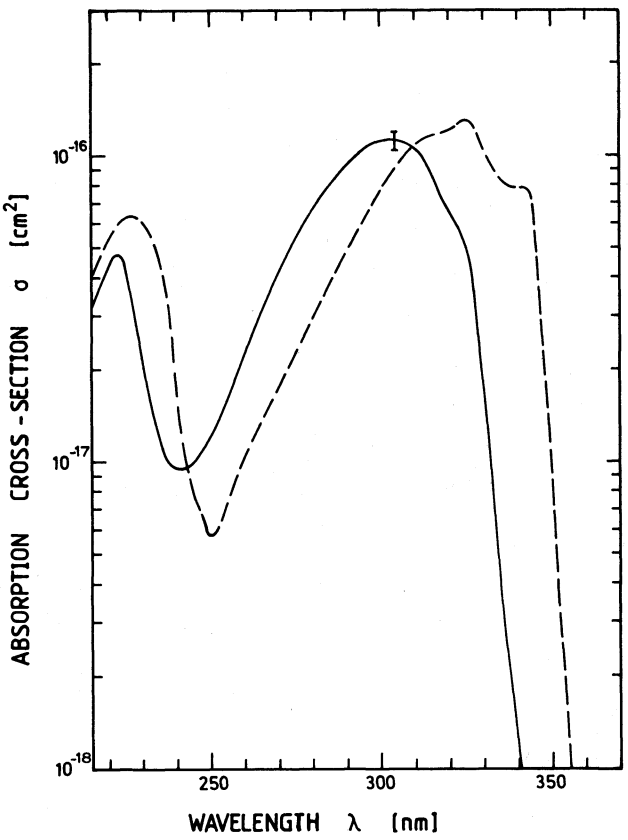

FIG. 6. Absorption cross-section spectra of PPF. Dashed curve, dye dissolved in cyclohexane (concentration 10^{-4} mol/dm^3). Solid curve, dye vapor at $\vartheta_R = 130$ °C ($\vartheta = 145$ °C).

respectively. The rise of absorption slows down above the saturation temperature ϑ_S (where $N_0 = N_S$). In the constant temperature regions the absorption decreases gradually, probably due to cell leakage, dye diffusion into pores of the cell walls, and dye decomposition. The calculated total absorption coefficients, $\alpha_0 = N_0\sigma$, for the amounts of dye inweighted are indicated.

The absorption cross-section spectrum of POPOP vapor at a reservoir temperature of $\vartheta_R = 250$ °C is shown by the solid curve in Fig. 5. The vapor spectrum is nearly independent of temperature in the investigated region between 200 and 300 °C. The absorption spectrum of POPOP dissolved in cyclohexane is shown by the dashed curve. The vapor spectrum is blue shifted and smoothed compared to the spectrum in cyclohexane.

The absorption cross-section spectra of PPF vapor ($\vartheta_R = 130$ °C) and of PPF dissolved in cyclohexane are shown in Fig. 6. Again the vapor spectrum is blue shifted and smoothed compared to the solution spectrum. Between 100 and 170 °C the vapor spectrum changes only slightly with temperature.

TABLE I. Dye parameters.

Dye	Dimethyl-POPOP	POPOP	PPF
Vapors			
$\lambda_{max}(S_0$–$S_1)$ (nm)	330	322	305
σ_{max} (cm^2)	1.6×10^{-16}	1.5×10^{-16}	1.12×10^{-16}
$\int_{S_0-S_1}\sigma(\tilde{\nu})d\tilde{\nu}$ (cm)	9.1×10^{-13}	1.09×10^{-12}	6.26×10^{-13}
ϑ_m (K)	505	515	361
Λ_s (J/mol)	1.5×10^5	1.4×10^5	1.02×10^5
Λ_e (J/mol)	1.2×10^5	1.1×10^5	7.4×10^4
Λ_m (J/mol)	3×10^4	3×10^4	2.8×10^4
Solutions			
Solvent	cyclohexane	cyclohexane	cyclohexane
$\lambda_{max}(S_0$–$S_1)$ (nm)	364	358	325
σ_{max} (cm^2)	1.9×10^{-16}	1.95×10^{-16}	1.3×10^{-16}
$\int_{S_0-S_1}\sigma(\tilde{\nu})d\tilde{\nu}$ (cm)	9.5×10^{-13}	1.13×10^{-12}	6.36×10^{-13}
$n(\lambda_{max})$[a]	1.4461	1.4472	1.4549
Data from comparison			
$\Delta\tilde{\nu}_{abs}$ (cm^{-1})	2830	3123	2018
J(cm^{-1})	1.34×10^4	1.48×10^4	1.13×10^4

[a] Extrapolated from Ref. 43.

The wavelengths of maximum S_0–S_1 absorption λ_{max}, the peak S_0–S_1 absorption cross-sections σ_{max}, and the integrated S_0–S_1 absorption cross-sections $\int_{S_0-S_1}\sigma(\tilde{\nu})d\tilde{\nu}$, ($\tilde{\nu}=\lambda^{-1}$) are listed in Table I. The S_0–S_1 absorption cross-section integrals of the dye vapors and the cyclohexane solutions are approximately equal.

The spectral shift of the absorption peaks of the solutions compared to the vapors was discussed in Ref. 7. For nonpolar solutes in nonpolar solvents the shift is caused by dispersion force interaction (London forces) and is given by[10]

$$\Delta\tilde{\nu}_{abs}=J\frac{n^2-1}{2n^2+1}, \tag{17}$$

J is a dye molecule dependent constant and n is the optical refractive index of the solution at its absorption peak. The obtained J values of the investigated dyes are listed in Table I.

B. Saturated vapor densities

The saturated vapor densities N_S are obtained from transmission measurements with surplus dye in the reservoir. N_S is given by $N_S=\alpha(\lambda)/\sigma(\lambda)$. The measured saturated vapor densities against temperature are shown by the data points of Figs. 7, 8, and 9, for POPOP, dimethyl-POPOP, and PPF, respectively.

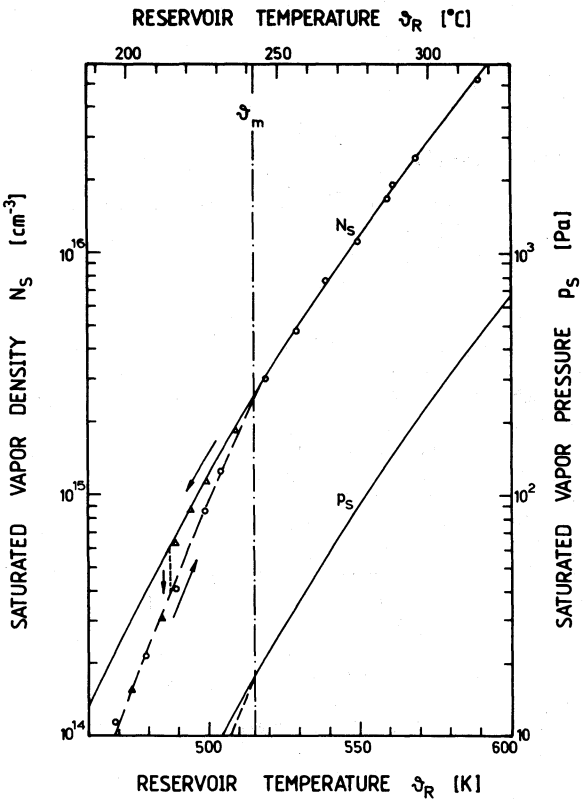

FIG. 7. Saturated vapor number density N_S and saturated vapor pressure p_S vs reservoir temperature for POPOP. Dashed–dotted line indicates melting temperature ϑ_m. Below ϑ_m circles indicate heating up and triangles indicate cooling down from above ϑ_m. Solid curves belong to dye evaporation ($Q_{des}=Q_e=1.77\times10^{-19}$ J, $\kappa_{des}=5.2\times10^{10}$ Pa K$^{-1/2}$, $\nu_{des}/S=3.6\times10^{15}$ s^{-1}). Dashed curves belong to sublimation ($Q_{des}=Q_s=2.28\times10^{-19}$ J, $\kappa_{des}=6.5\times10^{13}$ Pa K$^{-1/2}$, $\nu_{des}/S=4.5\times10^{18}$ s^{-1}).

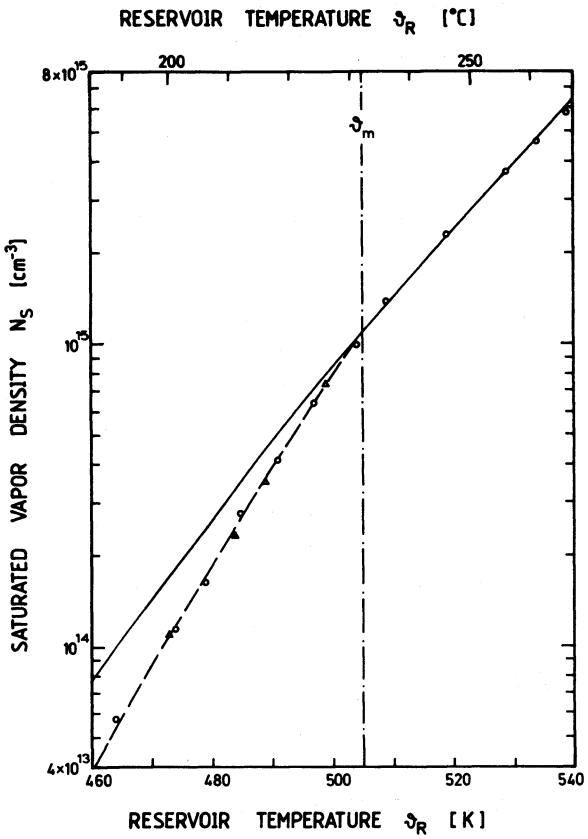

FIG. 8. Saturated vapor number density of dimethyl-POPOP vs temperature. ϑ_m is melting temperature. Below ϑ_m the circles belong to heating up and the triangles belong to cooling down from above ϑ_m. Solid curve is evaporation curve ($Q_{des}=Q_e=1.94\times10^{-19}$ J, $\kappa_{des}=3.9\times10^{11}$ Pa K$^{-1/2}$, $\nu_{des}/S=2.5\times10^{16}$ s^{-1}). Dashed curve is sublimation curve ($Q_{des}=Q_s=2.43\times10^{-19}$ J, $\kappa_{des}=4.6\times10^{14}$ Pa K$^{-1/2}$, $\nu_{des}/S=3\times10^{19}$ s^{-1}).

Reasonably high saturated vapor densities are obtained at temperatures where the dyes are still thermally stable. Therefore high stimulated emission gains may be obtained in dye vapor lasers with vapor cells of a few cm length.

The N_S curves in Figs. 7 to 9 are calculated [Eq. (12)] by fitting the constants κ_{des} and the desorption energies Q_{des} to the experimental points. The fitting parameters are listed in the figure captions. The curves depend exponentially on Q_{des} and linearly on κ_{des}. Therefore Q_{des} can be determined more accurately than κ_{des}. Assuming a desorption attempt frequency of $\nu_{des}=10^{13}$ s^{-1} and a dye surface density of $n_{surf}=2\times10^{18}$ m^{-2} the sticking coefficient may be determined (parameters are listed in the figure captions). In Figs. 7 (POPOP) and 9 (PPF) the calculated saturated vapor pressures p_S are included [Eq. (11)].

The theoretical curves in Figs. 7 to 9 fit to different Q_{des} values above and below the melting point of the dyes. Above the melting point the desorption energy Q_{des} is equal to the evaporation energy Q_e. Below the melting point Q_{des} is given by the sublimation energy Q_s. The energy difference $Q_m=Q_s-Q_e$ is the melting energy. The Q_e and Q_s values of the investigated dyes are listed in the figure captions.

Below the melting point the actual saturated vapor den-

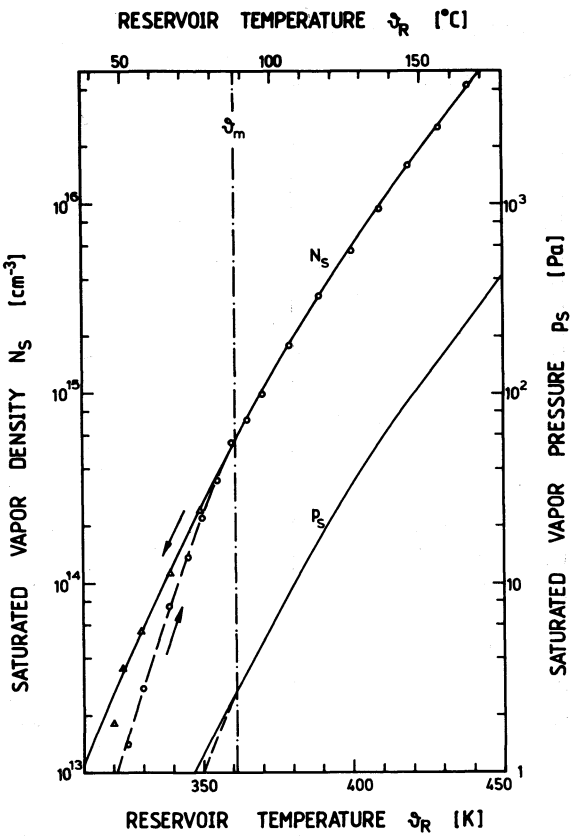

FIG. 9. Saturated vapor number density N_S and saturated vapor pressure p_S of PPF vs temperature. ϑ_m is melting temperature. Below ϑ_m the circles belong to heating up and the triangles belong to cooling down from above ϑ_m. Solid curves are evaporation curves ($Q_{des} = Q_e = 1.23\times10^{-19}$ J, $\kappa_{des} = 8.2\times10^9$ Pa K$^{-1/2}$, $\nu_{des}/S = 7\times10^{14}$ s^{-1}). Dashed curves are sublimation curves ($Q_{des} = Q_s = 1.69\times10^{-19}$ J, $\kappa_{des} = 8.8\times10^{13}$ Pa K$^{-1/2}$, $\nu_{des}/S = 7.7\times10^{18}$ s^{-1}).

sity depends on the vapor treatment. In the case of POPOP (Fig. 7) the saturated vapor pressure follows the sublimation curve when starting from temperatures below the melting temperature. In cooling down the POPOP dye from above the melting point, the experimental points continue to follow the evaporation curve down to nearly 30 °C below the melting point and then change over to the sublimation curve. It is thought that either supercooling of the liquid or an amorphous solidification of the dye occurs before at low enough temperatures the recrystallization of the dye occurs. If POPOP is heated up above 350 °C and kept at this high temperature for time durations longer than 1 h, then some dye decomposition occurs showing up in an increased short-wavelength vapor absorption in cooling down below 220 °C (not shown in Fig. 7).

The experimental saturated vapor density points of dimethyl-POPOP (Fig. 8) indicate no hysteresis effects (no supercooling in decreasing the temperature below the melting point). Only in the case of heating up the dye above 340 °C for about 1 h, then in cooling down below the melting point the experimental points continue to follow the evaporation curve (see Ref. 7).

The temperature behavior of the saturated vapor density of PPF is shown in Fig. 9. In heating up to the melting point the experimental points follow the sublimation curve. In cooling down from above the melting point the experimental data continue to follow the evaporation curve (no recrystalization). Down to 40 °C below the melting point no return to the sublimation curve is observed (last measured point at $\vartheta_R = 47$ °C gives some indication of beginning return).

C. Latent heats

The molar latent heats of sublimation Λ_s and evaporation Λ_e are proportional to the sublimation energies Q_s and evaporation energies Q_e [see Eq. (16)] which have been determined above by fitting the saturated vapor density equation (12) to the experimental points. The latent heats of melting Λ_m are obtained by $\Lambda_m = \Lambda_s - \Lambda_e$. The latent heats of the investigated dyes are listed in Table I. For comparison the molar latent heats of water are $\Lambda_s = 4.76\times10^4$ J/mol, $\Lambda_e = 4.16\times10^4$ J/mol, and $\Lambda_m = 6\times10^3$ J/mol.[42]

V. CONCLUSIONS

The dyes POPOP, dimethyl-POPOP, and PPF were analyzed by absorption spectroscopy. The absolute absorption cross-section spectra are determined. The blue shift of the vapor spectra compared to the liquid solution spectra allows to study the solvent influence. The temperature dependence of the saturated vapor density or the saturated vapor pressure allows the determination of the latent heats of sublimation, evaporation, and melting. The break in the vapor density curves determines the melting temperature of the investigated dyes.

ACKNOWLEDGMENT

The authors thank the Deutsche Forschungsgemeinschaft for financial support.

[1] *Topics in Applied Physics, Vol. 1, Dye Lasers*, 2nd ed., edited by F. P. Schäfer (Springer, Berlin, 1977).
[2] N. A. Borisevich and V. A. Tolkatchev, Sov. Phys. Uspeki **25**, 865 (1982).
[3] Yu. Yu. Stoilov, Appl. Phys. B **33**, 63 (1984).
[4] B. Steyer and F. P. Schäfer, Appl. Phys. **7**, 113 (1975).
[5] N. G. Basov, O. A. Logunov, A. V. Startsev, Yu. Yu. Stoilov, and V. S. Zuev, J. Mol. Struct. **79**, 119 (1982).
[6] J. P. Maier, A. Seilmeier, A. Laubereau, and W. Kaiser, Chem. Phys. Lett. **46**, 527 (1977).
[7] J. Schmidt and A. Penzkofer, Chem. Phys. **117**, 265 (1987).
[8] H. Weininger, J. Schmidt, and A. Penzkofer, Chem. Phys. **130**, 379 (1989).
[9] J. Schmidt and A. Penzkofer, Chem. Phys. **133**, 297 (1989).
[10] M. Mataga and T. Kubota, *Molecular Interactions and Electronic Spectra* (Dekker, New York, 1970), Chap. 8, p. 371.
[11] G. A. Abakumov, Yu. M. Anisimov, B. I. Polyakov, and A. P. Simonov, Appl. Phys. **23**, 83 (1980).
[12] G. A. Abakumov, S. A. Drobakha, A. V. Klimanov, A. V. Ostrovskii, B. I. Polyakov, and A. P. Simonov, Sov. J. Quantum. Electron. **16**, 1566 (1986).
[13] V. F. Lukinykh, S. A. Myslivets, A. K. Popov, and V. V. Slabko, Appl. Phys. B **38**, 143 (1985).
[14] V. F. Lukinykh, S. A. Myslivets, A. K. Popov, and V. V. Slabko, Sov. J. Quantum. Electron. **16**, 927 (1986).
[15] D. M. Khalimanovich, Appl. Spectrosc. (USSR) **36**, 411 (1982).
[16] A. N. Borisevich, G. B. Tolstorozhev, and D. M. Khalimanovich, J. Appl. Spectrosc. (USSR) **39**, 1019 (1984).

[17]A. P. Blokhin, V. A. Povedailo, and V. A. Tolkachev, Opt. Spectrosc. (USSR) **60**, 37 (1986).
[18]N. A. Borisevich, I. I. Kalosha, and V. A. Tolkachev, J. Appl. Spectrosc. (USSR) **19**, 1646 (1973).
[19]B. Steyer and F. P. Schäfer, Opt. Commun. **10**, 219(1974).
[20]Yu. Yu. Stoilov and K. K. Trusov, Sov. J. Quantum Electron. **4**, 809 (1974).
[21]P. W. Smith, P. F. Liao, C. V. Shank, T. K. Gustafson, C. Lin, and P. J. Maloney, Appl. Phys. Lett. **25**, 144 (1974).
[22]N. G. Basov, V. S. Zuev, Yu. Yu. Stoilov, and K. K. Trasov, Sov. J. Quantum Electron. **4**, 1178 (1975).
[23]P. W. Smith, P. F. Liao, C. V. Shank, C. Lin, and P. J. Maloney, IEEE J. Quantum Electron. **QE-11**, 84 (1975).
[24]G. Marowsky, F. P. Schäfer, J. W. Kato, and F. K. Tittel, Appl. Phys. **9**, 143 (1976).
[25]Yu. Yu. Stoilov, Sov. J. Quantum Electron. **5**, 1412 (1976).
[26]P. F. Liao, P. W. Smith, and P. J. Maloney, Opt. Commun. **17**, 219 (1976).
[27]Yu. Yu. Stoilov and K. K. Trosov, Sov. J. Quantum Electron. **7**, 216 (1977).
[28]V. S. Zuev, Yu. Yu. Stoilov, and K. K. Trusov, Sov. J. Quantum Electron. **7**, 247 (1977).
[29]G. Marowsky, R. Cordray, F. K. Tittel, W. L. Wilson, and C. B. Collins, Appl. Phys. Lett. **33**, 59 (1978).
[30]G. A. Abakumov, B. I. Polyakov, and A. P. Simonov, Opt. Spectrosc. (USSR) **45**, 752 (1978).
[31]T. Sakurai and A. Ogishima, IEEE J. Quantum Electron. **QE-15**, 506 (1979).
[32]G. Marowsky, G. P. Glass, F. K. Tittel, and W. L. Wilson, Chem. Phys. Lett. **67**, 243 (1979).
[33]G. A. Abakumov, Yu. M. Anisimov, P. I. Polyakov, and A. P. Simonov, Sov. J. Quantum Electron. **9**, 1337 (1979).
[34]N. A. Borisevich, S. A. Tikhomirov, and G. B. Tolstorozhev, Sov. Phys. Dokl. **28**, 37 (1983).
[35]K. K. Trusov, Opt. Spectrosc. (USSR) **57**, 358 (1984).
[36]T. F. Raichenok, J. Appl. Spectrosc. (USSR) **41**, 1217 (1984).
[37]G. A. Abakumov, S. A. Drobakha, V. B. Kolovskii, P. I. Polyakov, and A. P. Simonov, Sov. J. Quantum Electron. **15**, 393 (1985).
[38]L. M. Bolot'ko and A. A. Sukhodola, J. Appl. Spectrosc. (USSR) **46**, 73 (1987).
[39]G. A. Abakumov, S. A. Drobakha, A. V. Klimanov, A. V. Ostrovskii, B. I. Polyakov, A. P. Simonov, and L. S. Chuiko, Opt. Spectrosc. (USSR) **62**, 370 (1987).
[40]L. Eckertova, *Physics of Thin Films*, 2nd ed. (Plenum, New York, 1986), p. 99.
[41]P. W. Atkins, *Physical Chemistry*, 2nd ed. (Oxford University, Oxford, 1982).
[42]*American Institute of Physics Handbook*, 3rd ed., edited by D. E. Gray (McGraw–Hill, New York, 1972).
[43]*Landolt–Börnstein*, 6th ed., edited by K. H. Hellwege and A. M. Hellwege (Springer, Berlin, 1962), Vol. 2, Part 8.